ASSESSMENT OF A PARKING GARAGE WITH A BROKEN PRESTRESSED SPANDREL BEAM

Bishal Parajuli, EIT, Dept. of Civil Engineering, University of Toledo, USA
Seyedowjan Hashtroodi, EIT, Robert Darvas Associates, Ann Arbor, MI
Douglas K. Nims, PhD, PE, Dept. of Civil Engineering, University of Toledo, USA

ABSTRACT

A prestressed spandrel beam failed in a parking garage in Northwest Ohio. The 40 year old L shaped prestressed spandrel beam failed brittlely due to severe corrosion of the prestressing strands. A large crack occurred at the mid-span of the beam. The crack extended nearly to the top of the beam and the concrete above the crack spalled. Post failure visual inspection revealed few external indications of the extent of the corrosion. This paper discusses the failure and the visual inspection of the parking garage, analysis of the failed beam, and a trial magnetic flux leakage (MFL) inspection that was carried out to assess the potential of this technique in revealing the hidden corrosion in these spandrel beams..

The failed beam was prevented from falling because it wedged against the adjoining beams. The garage was immediately closed and all the remaining beams were visually inspected. Based on the visual inspection, a repair plan was executed. Linear and nonlinear analyses were carried out. The original design was found adequate, the cause of the failure was the deterioration of the prestressing strand and the MFL inspection found anomalies that were verified by excavation.

Keywords: Prestressed, Concrete, Corrosion, Failure, Repair, Magnetic Inspection

INTRODUCTION

In September 2013, an exterior prestressed spandrel beam in a parking garage in Northwest Ohio failed. The 40 year old L shaped prestressed spandrel beam failed brittlely and unexpectedly due to severe corrosion of the prestressing strands. A large crack occurred at the mid-span of the beam extending nearly to the top of the beam and the concrete above the crack spalled. The beam failed completely and was prevented from falling when the broken pieces wedged against the adjacent beams. Figure 1 shows the parking garage and figure 2 shows the crack. Post failure visual inspection revealed little external indication of the extent of the corrosion. After the failure, the garage was immediately closed and inspected. The garage was reopened after extensive repairs including strengthening of some spandrel beams and the addition of columns to shorten some beam spans.

Hidden corrosion in the strands of prestressed components is a problem which has attracted significant attention in the bridge industry (Jones 2010, Harries 2009). The literature review revealed no other instances of a parking garage beam failure due to non-visible corrosion.

This paper describes the parking garage, the failure, the remedial actions taken, analysis of the failed beams and a magnetic inspection of the prestressing in a sample of the beams.

DESCRIPTION OF THE PARKING GARAGE

The parking garage with the failed spandrel (which shall be referred to as the East Garage) was one of two that were built at the same time using the same design and materials. The garages were designed in April 1976 and constructed shortly thereafter and have been in continuous service since construction. The garage superstructure is constructed entirely of precast components including beams, columns and double tees. The failed beam was in the East Garage which has four parking levels. Level 1 is a concrete slab on grade. The other

three levels are elevated above it. The garage has a capacity of 1,050 vehicles and a rectangular footprint measuring 423 feet in the north-south direction and 177 feet in the east-west direction. The West Garage has three decks with the lower one resting on the grade and the other two above it. The concrete in the garages is expected to have a strength of approximately 5,000 psi. The prestressing strands have an ultimate strength of 250 ksi. The design specified a concrete cover of one inch.

The deck was composed of 24 inch deep by 9 foot wide double tees with a specified maximum deadload to 45 pounds per square foot. The double tees (DT's) were specified to have a 3 inch thick concrete topping. The deadload of the DT's plus topping was 82.5 pounds per square foot. The span of the double tees supported by the failed beam was 58 feet 0 inches. In some places, the double tees were severely deteriorated both at the joints between the tees and through the thickness of the flanges. On the exterior, the deck was supported by L-shaped spandrels and, in the interior, it was supported by inverted tee beams.

The failed spandrel was a typical exterior beam. It was at the fourth level on column line B and spanned 35 feet 10 inches between column lines 8 and 9. The beams had been cast and prestressed in Canada and shipped to the site. The exterior beams had a rope finish that left rough grooves approximately one inch deep on the outer face.

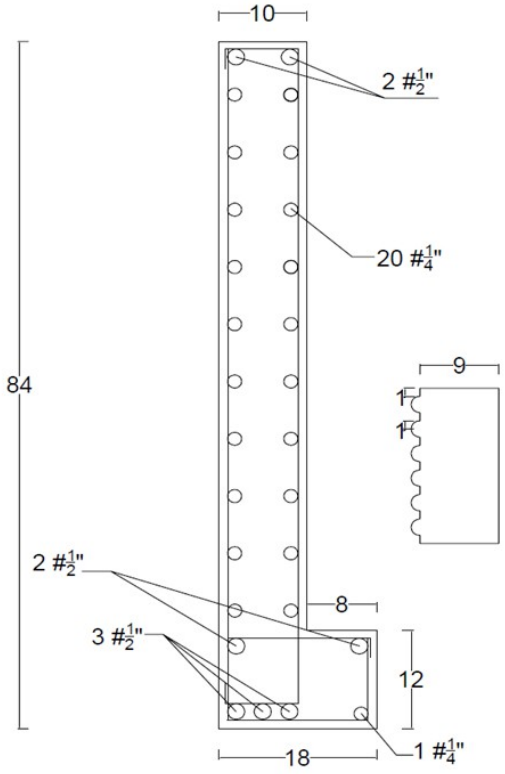

Figure 3 shows the cross section of the spandrel. Figure 4 shows a detail of the 10 inch width of the stem which consists of 9 inches of solid section and 1 inch of grooved exterior. The longitudinal reinforcement in the section consists of 28 prestressing strands: seven one-half inch prestressing strands and 21 one-quarter inch strands. There was no conventional longitudinal reinforcing steel. At the mid-span of the beam, where the crack occurred, there are number 4 bar vertical stirrups at twelve inch spacing.

DESCRIPTION OF THE FAILURE

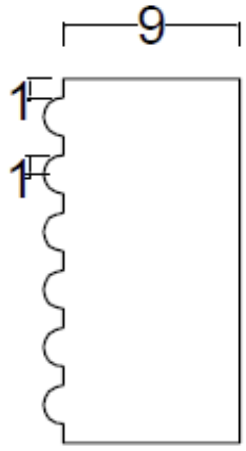

Figures 5 and 6 show the interior and exterior details of the crack. Note in Figure 5, the concrete is spalled at the top of the crack. In Figure 6, evidence of water leaking through the deck joint near the crack location can be observed. Figure 7 shows the crack extending upward from the deck to within a few inches of the top of the beam. Note the repairs in the deck joint near the crack indicating a history of leakage. The failure surface was inspected thoroughly. Even through small cracks could be easily observed on the painted interior surface, there was no sign of any distributed small cracks near the main crack, which would normally form in a ductile failure. There was only one dominant crack which had propagated through the depth of the beam at the mid-span. This is evidence of a brittle flexural failure.

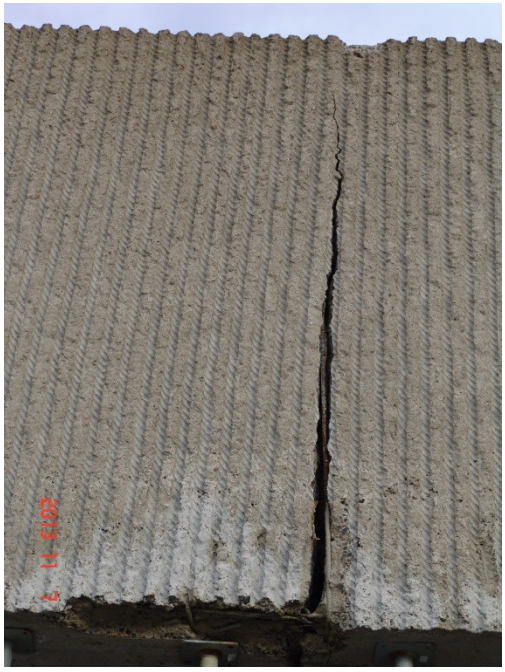

The crack was approximately two inches wide at the bottom of the beam. Viewed from inside the garage and from the top deck there was an easily visible kink in the beam. Inspecting the joint between the failed beam and the adjacent beams, it was clear the failed beam had broken into two pieces which had rotated as rigid

bodies. The downward motion had been arrested due to arch action with the top midspan of the beam in compression between the failed pieces and the lower corners of the broken beam pressed against the adjacent beams. The portion of the beam that the column was attached to had a smooth surface. The beam had rotated until the protruding rope roughened surface had come to rest against the column. The rough texture of the column may have inhibited further rotation and caused tension in the bolts designed to resist torsion in the spandrel. Thus, it is possible the rough texture of the exterior face prevented the collapse.

Figures 8 and 9 show details of the ½ inch strand breaks at the crack. In figure 3, this is the lowest level of strand below the stem. The outer two ½ inch strands are severely corroded with the outermost one essentially having completely dissolved. The inner most ½ inch strand also has extensive rusting. The ¼ inch strand in the bottom of the ledge could be felt, but not clearly inspected visually. The vertical face of the flange on the interior of the garage is painted white and cracks are easy to observe. However, in the region of the dominant crack, no cracks adjacent to the main crack were observed on the vertical face and there was no visible signs such as spalling, efflorescence or discoloration of the concrete on the bottom of the beam.

There was no reported direct visual or aural observation of the beam breaking. It was assumed to have broken before or after a

sporting event that occurred the day before the failure was reported. The demand on the beam at the time of failure would have been the deadweight of the beam, the deck and the topping plus the live load. There were no significant utilities attached to the failed beam. For estimating the maximum demand, the live load was considered as 40 psf. Assuming the garage was loaded when the beam failed, unfactored moment demand at midspan was approximately 700 kip-feet.

INSPECTION AND REPAIR

To assess the state of the East Garage and its companion, a thorough visual and tactile inspection of parking garages was carried out by a team from Poggemeyer Design Group (PDG). Material testing was also conducted. Chloride content was found to be within normal limits. For the beams, the result of this inspection was a crack map. The cracks on the interior bottom face of the beams were observed and rated on the basis of the severity of the cracks. Most of the cracks were hairline, however, hairline cracks that appeared to go through the flange or extend to the top are potentially significant. The closer the crack ran to the top of the beam, the higher the rating assigned to it. Cracks that ran the entire depth of the interior flange were assigned a 10 and cracks that ran up 50% of the flange depth were assigned a 5 and so forth. The exterior condition of the beam was also considered. In some instances, there was a significant loss of concrete section and the tendons were exposed (Figure 10). The exposed strand and stirrups revealed that in some instances the cover was less than the 1 inch shown on the drawings and the concrete was porous. Overall, the visual inspection gave an estimate of the condition of the beams.

Immediate repairs were carried out to make the garage safe for use. Based on the severity of the cracks and the surface condition, various repair actions were taken. The beams with maximum cracking were rehabilitated by adding new columns (Figs 11 and 12), moderately cracked beams with no head room restrictions were reinforced with external post-tensioning (Fig 13) and the beams which showed minimal cracking or had headroom restrictions were wrapped with carbon fiber. Nine new columns were installed in the East Garage. These columns were installed at midspan and extended from the ground to the top. The foundations for the

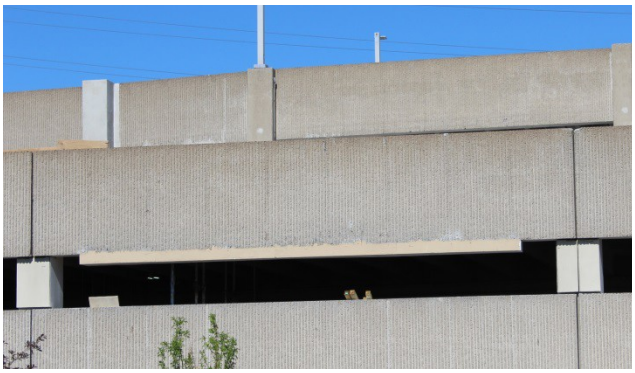

new columns were an array of small drilled piles.

Repair recommendations were also made for the deck and repairs were carried out in the summer of 2015 and additional deck repairs are ongoing in the summer of 2016 (Fig 14).

ANALYSIS

In order to further investigate and understand the sudden failure of the spandrel beam, it was decided to perform several analyses of the beam. Three approaches were used: preliminary hand calculations were performed to compute the ultimate moment capacity and the cracking moment of the beam based on the ACI 318 – 11, Response 2000 (Bentz 2001) was used for sectional analysis of the beam and cracking response, and ABAQUS (Abaqus 2014) was used

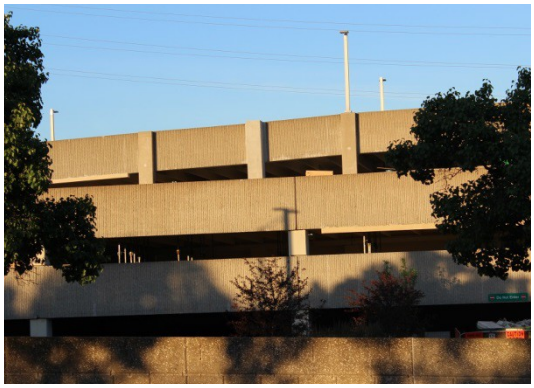

to perform a 3D finite element analysis to further investigate the crack propagation through the depth of the beam. The hand analyses give a basic feel for the behavior and provide a reasonableness check for the computational results. For the undamaged model, the design appeared reasonable the span to depth ratio is appropriate and the serve stress under the full design load at the bottom of the beam was 130 psi tension. In all the approaches, damage was simulated by removing strands from the model, i.e., the undamaged model and models with 1, 2, 3 and 4 strands were removed. The full and damaged models were used to calculate the ultimate and cracking moment at the section. The goal of the analyses was to check if the observed strand loss and condition of the beam is consistent with the observed failure.

The modulus of rupture suggested for design is . However, according to the authors' test experience and ACI 363R, this value is the lower limit of the modulus of rupture, therefore, it is not accurate for estimating failure loads. The value of modulus of rupture can vary between and . Values of and . were used in the analyses to better capture and simulate the actual behavior of the beam. The strength of the concrete used in the analysis was 5,000 psi.

ACI 318-11 states, if the ratio of ultimate moment capacity to cracking moment exceeds 1.2, then the structure should be ductile enough to undergo considerable deflection before failure. For the purpose of this analysis, brittle failure was assumed to occur if this ratio was approximately 1.

In order to calculate the cracking moment of the cross section, Eq. 5-4 in the PCI Design Handbook 7th Edition was used. The final beam is not a composite section so the equation reduces to

where

e = eccentricity of the force
f_r = modulus of rupture
M_{cr} = cracking moment
P = force in the prestressing after losses
S_b = section modulus

For calculating the cracking moment, 25% long term losses were assumed.

Based on hand calculations, the as designed beam, i.e. with no damage to the structural elements, such as tendons, concrete, etc., was strong and ductile enough that no abrupt failure should occur after cracking happens. Therefore, the beam should tolerate additional load and undergo considerable deformation before ultimate strength is reached and the beam fails. The difference between the ultimate moment capacity calculated by Reponse2000 and hand

calculations is less than 1%. In order to estimate the cracking moment, the moment-curvature plot was used (Hashtroodi 2015).

Response 2000 was used to do a sectional analysis in accordance with the modified compression field theory. For each damage scenario, the ultimate moment capacity over the cracking moment ratio was calculated to estimate the number of corroded strands needed for the beam to experience brittle failure. Crack patterns throughout the length of the beam and the existence of a dominant macro-crack was also studied and compared to the observed failure. Response 2000 calculated that with the brittle failure of the beam occurs when1.75 half-inch tendons have been broken. This number of broken tendons corresponds well to the loss of tendon cross section observed in the failed beam (Hashtroodi 2015).

The crack plots in Response 2000 were used to study the behavior of the beam as the strands were removed. The plots provided insight into how and when the distributed cracks associated with ductile behavior transformed into the single dominant brittle failure crack as the behavior switches from ductile to brittle as tendons are removed one by one from the bottom layer of the beam. Furthermore, the crack widths of distributed cracks tend to decrease, however, at the same time, the width of one dominant macro-crack at mid-span increases as each tendon is removed from the beam (Hashtroodi 2015).

A three-dimensional finite element model of the pre-stressed parking garage beam was created by use of SolidWorks and ABAQUS software to further study the crack propagation. One initial crack was defined at mid-span of the beam by modelling a cohesive segment surface which would allow the crack to open up and propagate through the depth of the beam when the stress exceeds the corresponding limit under the applied loading. In order to investigate the strands effect on crack propagation and behavior of the beam, two bottom-layer strands were modelled as broken strands - to simulate the existing condition of the failed beam. The beam was modelled by defining three different individual parts. First, the concrete was modelled as a whole “3D deformable extrusion solid” element. For creating the tendons, “3D deformable planar wire” elements were used. For crack propagation of the beam, another separate part was defined to act as the initial crack of the beam. The crack was modelled using “3D deformable extrusion shell” with 8 inches of extrusion (Hashtroodi 2015).

The crack propagation of the beam at a few stages before complete failure is presented in the figure 15. It can be observed that at this stage, the crack has propagated through the depth of the beam and the crack tip is at the compression zone of the beam. Comparing figures 2 and 15 – the analysis and actual crack patterns are similar.

The analyses confirmed that the observed strand loss and condition of the beam is consistent with the observed failure. All of the three analytical approaches gave results that were consistent with each other and the observed damage to the beam. The analyses indicate that the beam was initially designed with adequate ductility and capacity and the deterioration of approximately two strands would be sufficient to enable brittle failure. The cracking moment capacity of the intact section is significantly greater than the likely load at failure. A crack approximately 7 inches long would reduce the cracking moment capacity to the estimated demand at the time of failure.

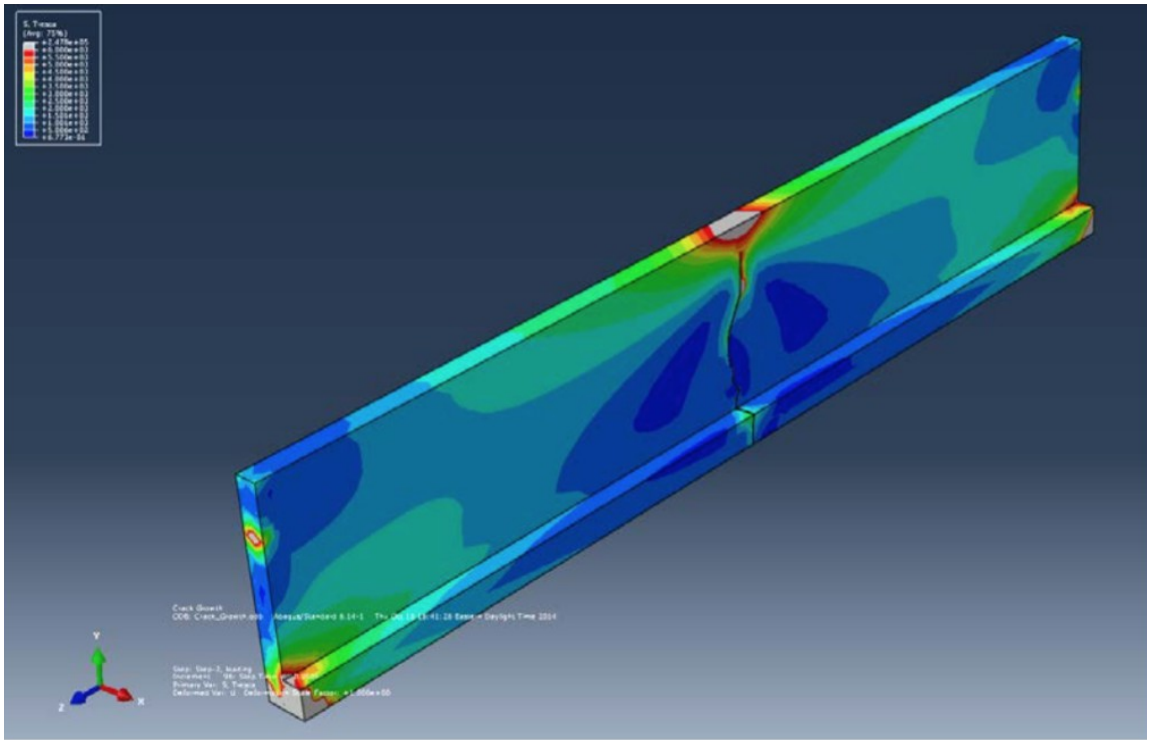

MAGNETIC INSPECTION

A trial of magnetic flux leakage (MFL) inspection was conducted on seven beams in the East Garage. MFL has been shown to be a promising nondestructive way to investigate invisible corrosion in prestressing strands (Ghorbanpoor 2000, Fernandes 2013A, 2013B, Harries 2009). There are several hundred prestressed beams in the two garages and a way to nondestructively evaluate the condition of the strand would be a valuable supplement to visual inspection. Statistically this is a very small sample and is more a proof of concept than an inspection. This test was done in collaboration with a team from The University of Wisconsin, Milwaukee led by Prof. Ghorbanpoor.

In MFL, a constant directional flow of magnetic flux is generated in prestressing strands when an external magnetic field is applied. If the strand has a flaw due to corrosion, some or all of the flux leaks out of the strand. This leakage is detected by Hall Sensors and produce signals with different amplitude compared to the normal flux signal. (Harries 2009). The technique is discussed in detail by Ghorbanpoor and Fernandes (Ghorbanpoor 2010, Fernandes 2012)

MFL is particularly well suited to this application because it uses a permanent magnet which is much lighter than the electromagnets required by the main flux and residual magnetism methods. The magnet and Hall-effect sensors and mounted on robotic beam traveler which can hang from the lower flange of the beam. The movement of this beam traveler can be controlled from the ground. As it travels along the length of the beam, it scans the condition of steel strands inside the beam. As the traveler scans, the flux data is acquired by a PC based data acquisition system. A graph of the data is displayed to the operator as it is acquired. The sensors can cover only half width of the beam so two passes had to be made. Thus, for a particular beam, the full width scan result comprises of the scan result of east half and west half. As can be seen in figure 16, the tires of the robotic beam traveler gripped the exterior faces of the beam while it moved. The wheels are angled upward to keep the traveler from slipping down.

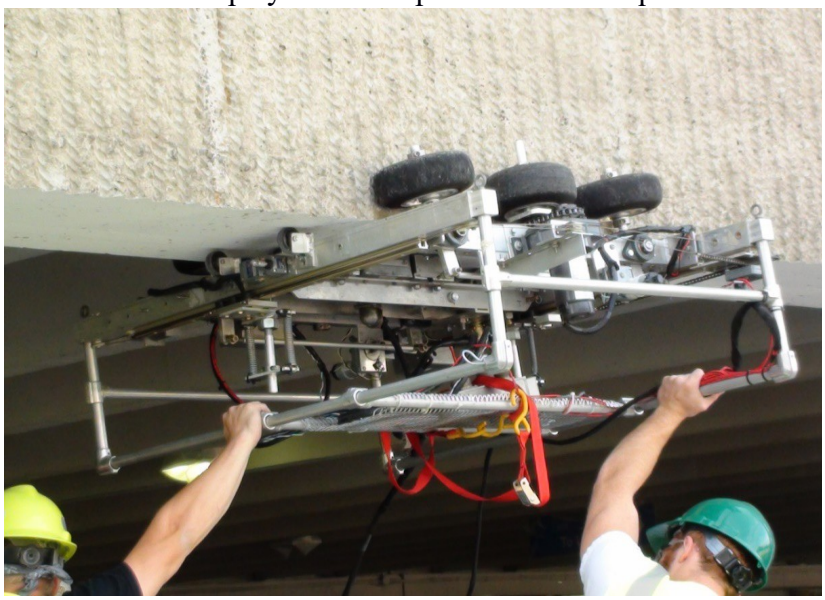

The beams considered for the magnetic test were chosen by

visual inspection of the physical condition of the beam. Two of the selected beams were control beams that had no visible cracking. The other five beams were selected by indications of potential damage including visible cracking or a history of repair due to cracking. The beams are numbered to correspond to their position in the parking garage. The beam designation was X-Y-ZCD where the beam runs north south from column X to column Y on level Z along column line C and if there are two beams at that location the D indicates whether it is the east or west beam. For example, beam 8-9-4CW is the western beam running between columns 8 and 9 along column line C on the 4th level. The beams selected to be scanned are given in Table 1.

Table 1 Beams Selected for Magnetic Inspection

Parking Level	Name of beam	Condition
2	11-12-1A	Uncracked
2	11-12-1C	Uncracked
4	5mid-6-4CW	Small crack
4	5-5mid-4CW	Small crack
4	8mid-9-4B	Distortion in shape
4	8-8mid-4B	Distortion in shape
4	8-9-4CW	Potentially significant crack

Overall, the MFL results showed some small anomalies, but no evidence of major corrosion. Significant corrosion leaves a clear signature (Fernandes, 2012 and Ghorbanpoor 2010), but no such indications were found. Three beams were excavated to confirm the results of the magnetic inspection. The amplitude (peak) of the graph marked the presence of transverse stirrup and the distance between two regular peaks indicated the distance between the stirrups in the beam (Fernandes, 2012). Any irregularity in the signal implied the presence of corroded bar or a wrongly placed stirrup. The results for two of the excavations will be discussed here. Figure 17 shows the results from beam 5mid-6-4CW. The red circle designates an anomaly.
Upon evacuation, the strand was found to be sound and it was determined that the anomaly was caused by an extra piece of steel in the beam.

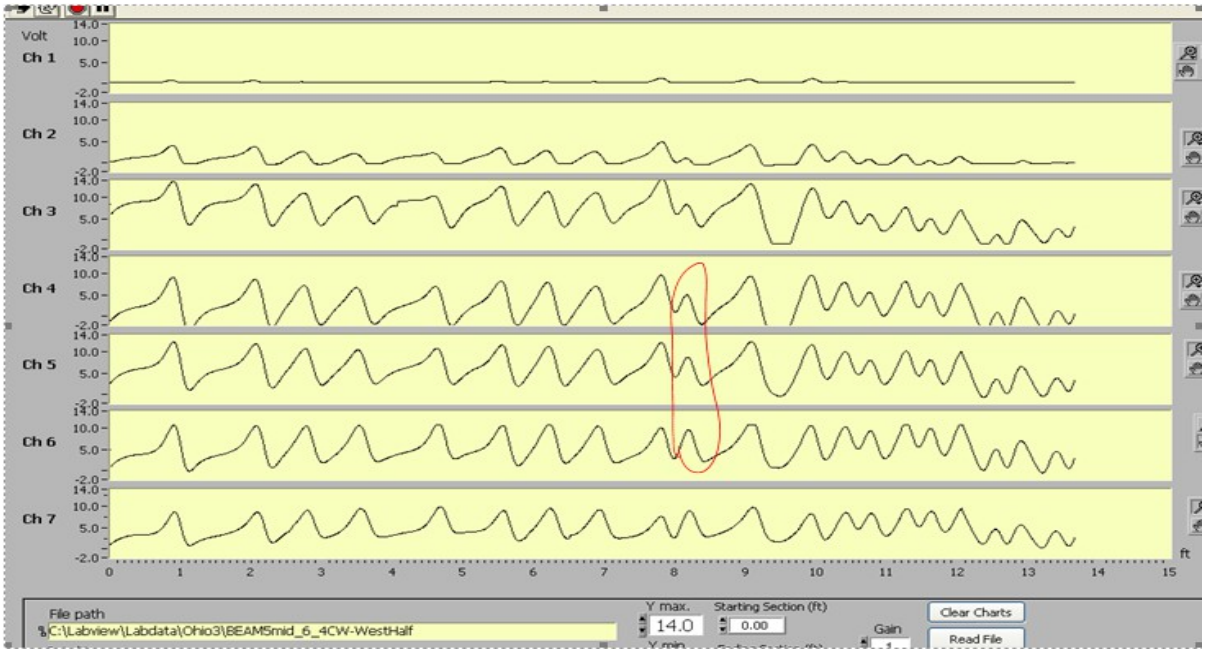

Beam 8-9-4CW had a potentially significant crack. This crack, which wrapped around the flange of the spandrel, was observed by the PDG project manager to be opening and closing with temperature. Because the crack was active, the beam was externally post-tensioned before the strand was evacuated. The crack was visible in the region between 18’ and 19.5’ as marked in figure 18, which shows the region that was excavated. In this figure, the white region is the existing spandrel and the unpainted region is the concrete covered for the external post tensioning. The MFL scan (Figure 19) suggests that the strands in the region of the crack may have some minor general corrosion. The anomalous region is circled. Note that since the scan results are offset by 2’, the crack region falls between 16’ and 17.5’ on the scan plot.

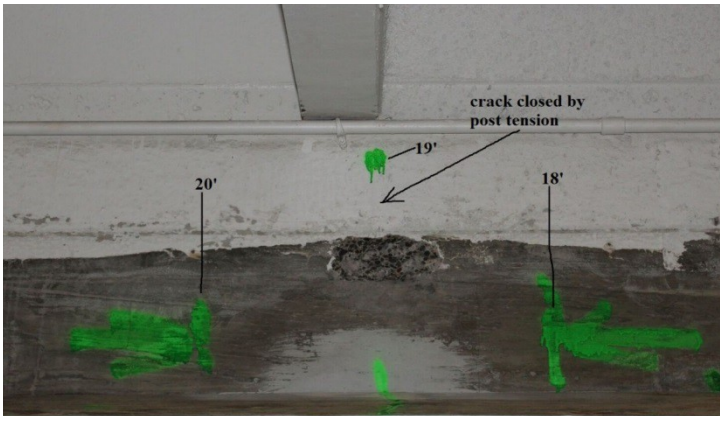

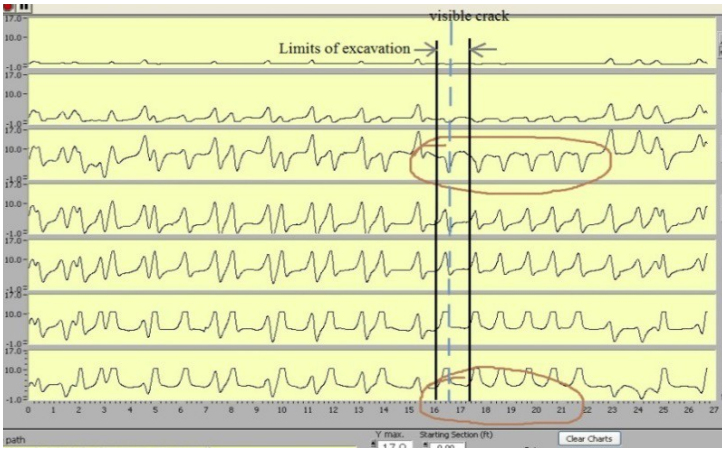

Upon excavation, the condition of the strands was found to be healthy with no visible corrosion (figure 20). The concrete in the excavation was tested with phenolphthalein. This pH test confirmed that the concrete still had a pH above 12 so the passivating layer was intact. This is consistent with the condition of the strand showing no trace of corrosion.

Because no significant indications of corrosion were found in any of the magnetic inspections and all the areas excavated revealed sound concrete and healthy strands, it was decided not to conduct any further excavations.

Overall, the causes of the anomalies indicated by the magnetic inspection were found for two of the three beams excavated. Table 2 summarizes the excavation results.

Table 2: Comparison of MFL and excavation result

Beam	MFL result	Excavation result
11-12-1A	anomaly in the location 16 to 18 feet from the face of column 11	A misplaced stirrup at the location of the anomaly
5mid-6-4CW	anomaly in the location 10 to 12 feet from the face of column 6	Extra piece of steel was left in beam
8-9-4CW	anomaly in the location 17 to 24 from the face of column 8	Strands were healthy and no extra steel was found

CONCLUSION

This paper reports the failure of a prestressed spandrel beam in a parking garage, the ensuing inspection and repair of the garage, the analysis of the beam in the initial and damaged condition and a trial magnetic inspection that examined the condition of some strands in-situ. These inspections and calculations lead to a likely failure scenario.

After the failure, the garage was thoroughly inspected and material tests were carried out. Based on these, repairs to the beams have been completed and repairs to the deck are underway. Hand, 2D modified compression field sectional analysis and 3D crack propagation analyses were completed. The analyses indicate the initial design had adequate strength and ductility, predict brittle failure when the beam deterioration is consistent with the observed corrosion and show crack patterns similar to the observed cracks. Magnetic inspection was carried out on a sample of seven beams. Statistically this is a very small sample. No significant corrosion was found.

Because there is no direct evidence or analytical verification of the failure mode, the failure scenario requires some speculation. The physical inspection showed cracks occurred in the beams with some regularity. The magnetic inspection showed that where there is no disturbance of the passivating layer the strand is in good condition. The analysis indicates the beam likely failed at a load less than the nominal cracking load. Therefore, it seems probable there was an initial crack that formed in the failed beam and the joint near the crack directed some water into the crack leading to the local deterioration of strand. This lead to corrosion which caused a loss of prestressing area equivalent to the loss of approximately two strands. This was sufficient strand loss to trigger a brittle failure. This scenario is consistent with the failure mode, leakage through the deck, corrosion of the strand and analytical results.

However, it is inconsistent with this hypothesis that there was not a sign of water exiting the spandrel at the crack location or of rust strain near the corroded strands.

ACKNOWLEDGEMENTS

Mr. Tom Stuckey of Poggemeyer Design Group (PDG) was the project manager of the rehabilitation and helped us throughout the experimental phase. The authors routinely had productive discussions with Mr. Stuckey concerning parking garage design and behavior. Mr. Phil Whaley, P.E., partner of PDG, provided guidance and support from the beginning of the project.

University of Toledo Facilities and Construction team has provided invaluable support including funding the magnetic inspection. These include Mr. Doug Collins, Director, Grounds and Transportation who provided direction and essential administrative support, Mr. Dan Klett, Director, Campus Planning and Design, who helped throughout the project, and Mr. Xiaozhong Zhang, FIS Database Analyst, who provided gracious assistance locating and reviewing the original drawings of the East Parking Garage.

Prof. Al Ghorbanpoor of the University of Wisconsin, Milwaukee provided the equipment and expertise for the magnetic inspection.

The authors and the readers owe a debt to Ms. Christine Lonsway who edited this paper.

REFERENCES

Abaqus Unified FEA, 2014, Dassault Systèmes, http://www.3ds.com/products-services/simulia/products/abaqus/latest-release/

American Concrete Institute Committee 318, 2011, "Building Code Requirements for Structural Concrete and Commentary," ACI 318-11, Farmington Hills, MI, pp. 503.

American Concrete Institute Committee 363, 2010, "Report on High-Strength Concrete," ACI 363R-10, Farmington Hills, MI, pp. 65.

Bentz, E. and M. Collins, 2001, Response 2000, University of Toronto, Toronto, Ontario Canada

Fernandes, B., D. Nims and V. Devabhaktuni, 2013A, "Computer aided modeling of magnetic behavior of embedded prestressing strand for corrosion estimation," *Journal of Nondestructive Evaluation*, June, Volume 32, Issue 2, pp.124-133.

Fernandes, B., M. Titus, D. Nims, A. Ghorbanpoor, and V. Devabhaktuni, 2012 "A Field Test of Magnetic Methods for Corrosion Detection in Prestressing Strands in Adjacent Box-Beam Bridges", Technical Note in *ASCE Journal of Bridge Engineering*. Nov/Dec. V. 17, No. 6, pp. 984 - 988.

Fernandes, B., M. Titus, D. Nims, A. Ghorbanpoor, V. Devabhaktuni, 2013B, "Practical Assessment of Magnetic Methods for Corrosion Detection in an Adjacent Precast, Prestressed Concrete Box-Beam Bridge", *Nondestructive Testing and Evaluation*, V. 28, No. 2,pp. 99-118.

Ghorbanpoor, A., 2010, "MFL Tests at P/S Concrete Box Girder Bridge Washington-Waterloo Rd, Fayette Co., Ohio", Summary Report for The University of Toledo, Toledo, Ohio.

Ghorbanpoor, A., R. Borchelt, M. Edwards, and E. Abdel Salam, 2000, "Magnetic Based NDE of Prestressed and Post Tensioned Concrete Members – The MFL System, Report FHWA-RD-00-026, May

Harries, K., 2009, "Structural Testing of Prestressed Concrete Girders from the Lake View Drive Bridge", *ASCE Journal of Bridge Engineering* Vol. 14, No. 2, pp 78-92.

Hashtroodi, S., 2015, *Crack Propagation Analysis of a Pre-stressed L-shaped Spandrel Parking Garage Beam*, Master's Thesis, University of Toledo, May 2015. https://etd.ohiolink.edu/!etd.send_file?accession=toledo1420753991&disposition=inline

Jones, L., Pessiki, S., Naito, C. and Hodgson, I, 2010,. "Inspection methods & techniques to determine non visible corrosion of prestressing strands in concrete bridge components, Task 2 – Assessment of candidate NDT methods." ATLSS Report No. 09-09, Lehigh University, Bethlehem, PA and Pennsylvania Department of Transportation, Harrisburg, PA.

Parajuli, B., 2016, *Study of Hidden Corrosion on Prestressing Strands*, Master's Thesis, University of Toledo, May. (available at OhioLink.edu shortly)

PCI Industry Handbook Committee, 2010, *PCI Design Handbook* 7th Edition, Prestressed/Precast Concrete Institute, Chicago, Il